

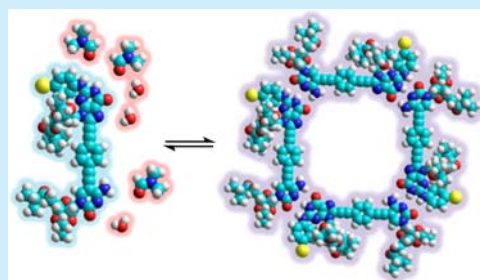
# G-Arylated Hydrogen-Bonded Cyclic Tetramer Assemblies with Remarkable Thermodynamic and Kinetic Stability

Sonia Romero-Pérez, Jorge Camacho-García, Carlos Montoro-García, Ana M. López-Pérez, Alfredo Sanz, María José Mayoral, and David González-Rodríguez\*

Nanostructured Molecular Systems and Materials Group, Departamento de Química Orgánica, Universidad Autónoma de Madrid, 28049 Madrid, Spain

**S** Supporting Information

**ABSTRACT:** The preparation and self-assembly of novel G–C dinucleoside monomers that are equipped with electron-poor aryl groups at the G–N<sup>2</sup> amino group have been studied. Such monomers associate via Watson–Crick H-bonding into discrete unstrained tetrameric macrocycles that arise as a thermodynamically and kinetically stabilized product in a wide variety of experimental conditions, including very polar solvent environments and low concentrations. G-arylation produces an increased stability of the cyclic assembly, as a result of a subtle interplay between enthalpic and entropic effects involving the solvent coordination sphere.



Macrocycles are aesthetically appealing chemical structures that offer manifold possibilities in diverse fields.<sup>1</sup> Shape-persistent covalent macrocycles, as well as their organized 2D porous networks<sup>2</sup> or 1D stacked nanotubes,<sup>3</sup> have been employed in organic electronics,<sup>4</sup> inclusion chemistry, sensing and catalysis,<sup>5</sup> rotaxane and catenane assembly,<sup>1</sup> or as nanomembranes and synthetic ion channels.<sup>6</sup>

As opposed to covalent methods,<sup>1,4,7</sup> noncovalent synthesis can be viewed as a straightforward and versatile approach toward well-defined macrocycles.<sup>8</sup> The idea is simple: one or several monomers are equipped with supramolecular motifs that contain the information to self-assemble in a single cyclic structure under thermodynamic control. However, the resulting supramolecular macrocycles are not as robust and persistent as their covalent analogues and achieving complete selectivity is a challenging task that demands careful molecular design.<sup>9</sup> Unbound monomers, noncyclic oligomers, or other cyclic structures often compete with the targeted macrocycle, and the relative weight of each species is highly sensitive to the experimental conditions: solvent, concentration, and temperature. Ideally, in order to reach close to quantitative amounts of a given cyclic structure, one should maximize the strength of the intermolecular interactions, as well as minimize the strain generated upon cyclization and the possibilities for alternative monomer conformations.

We recently described<sup>10</sup> the preparation of discrete H-bonded cyclic tetramers<sup>11,12</sup> (Figure 1) from a rigid monomer ( $\text{GC}_\text{H}$ ) that is substituted with complementary nucleosides,<sup>13</sup> guanosine (G) and cytosine (C), at both termini.<sup>10</sup> Watson–Crick G–C H-bonding pairing affords an unstrained square-shaped assembly with high fidelity in a broad number of experimental conditions. Here, we extend our studies to related monomers ( $\text{GC}_\text{Ar1}$  and  $\text{GC}_\text{Ar2}$ ) in which we introduce *p*-substituted electron-poor aryl groups at the G–N<sup>2</sup> via palladium-

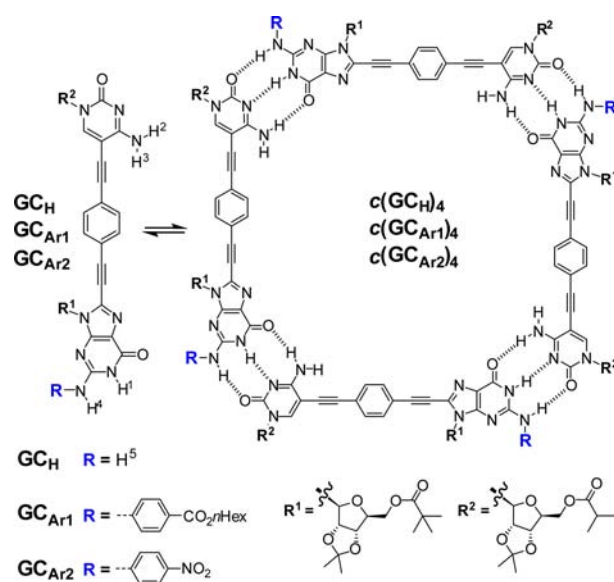


**Figure 1.** Chemical structure of monomers  $\text{GC}_\text{H}$ ,  $\text{GC}_\text{Ar1}$ , and  $\text{GC}_\text{Ar2}$  and their corresponding cyclic tetramer assemblies  $c(\text{GC}_\text{H})_4$ ,  $c(\text{GC}_\text{Ar1})_4$ , and  $c(\text{GC}_\text{Ar2})_4$  studied in this work.

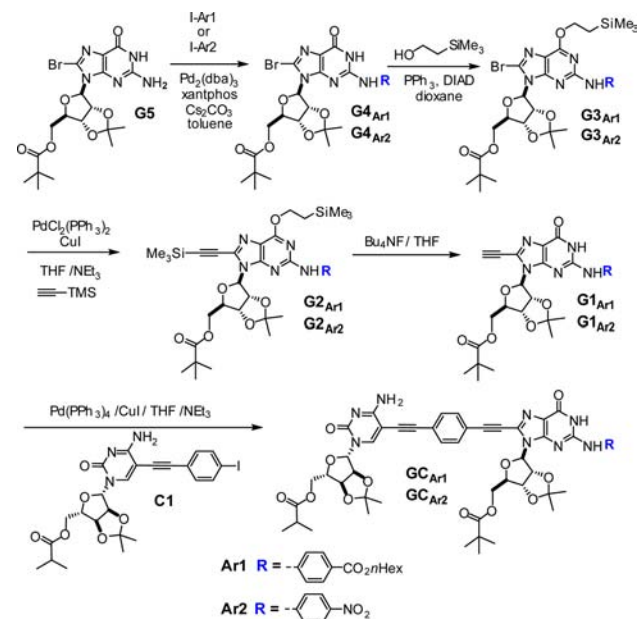
catalyzed C–N cross-coupling. The objective of this monomer modification is to enhance the stability of the cyclic assemblies by increasing the H-bonding donor ability of the G-amino proton. The resulting tetrameric macrocycles exhibit an impressive thermodynamic and kinetic stability and are able to persist even in highly polar solvent environments.

Received: April 10, 2015

Published: May 12, 2015

The synthesis of  $\text{GC}_{\text{Ar}1}$  and  $\text{GC}_{\text{Ar}2}$  followed a similar route to that reported for  $\text{GC}_{\text{H}}$  (Scheme 1).<sup>10,14</sup> The key palladium-

### Scheme 1. Synthesis of Monomers $\text{GC}_{\text{Ar}1}$ and $\text{GC}_{\text{Ar}2}$



catalyzed *N*-arylation<sup>15</sup> with the corresponding iodoarenes was essayed over different G substrates, trying to achieve the most straightforward synthetic path.<sup>16</sup> The best results were obtained when performing the reaction on G5,<sup>14</sup> leading to *N*-arylated compounds  $\text{G4}_{\text{Ar}1}$  and  $\text{G4}_{\text{Ar}2}$ . Due to the low reactivity of bromoguanosines,<sup>17</sup> the oxidative addition is fully selective on the iodoarenes at this step. The G-carbonyl group of these products was then protected as a trimethylsilyloxy moiety in order to carry out the Sonogashira reaction on  $\text{G3}_{\text{Ar}1}$  and  $\text{G3}_{\text{Ar}2}$ .<sup>17</sup> Deprotection of the silyl groups of  $\text{G2}_{\text{Ar}1}$  and  $\text{G2}_{\text{Ar}2}$  in the presence of tetrabutylammonium fluoride afforded  $\text{G1}_{\text{Ar}1}$  and  $\text{G1}_{\text{Ar}2}$ , which were then subjected to another palladium-catalyzed coupling with the 5-substituted pyrimidine nucleoside C1, whose synthesis has been recently reported by us.<sup>10,14</sup> This reaction led to final monomers  $\text{GC}_{\text{Ar}1}$  and  $\text{GC}_{\text{Ar}2}$ . All compounds were characterized by  $^1\text{H}$  NMR,  $^{13}\text{C}$  NMR, MS, and HR-MS techniques.<sup>16</sup>

Solutions of  $\text{GC}_{\text{H}}$ ,  $\text{GC}_{\text{Ar}1}$ , or  $\text{GC}_{\text{Ar}2}$  ( $10^{-1}$  to  $10^{-3}$  M) in nonpolar solvents, such as  $\text{CDCl}_3$ ,  $\text{CDCl}_2\text{CDCl}_2$ ,  $\text{CD}_2\text{Cl}_2$ , or  $\text{THF-D}_8$ , resulted in  $^1\text{H}$  NMR spectra that revealed a single set of proton resonances which are characteristic of G–C association (Figures 2a and S1). The H-bonded G–H<sup>1</sup> amide and the C–H<sup>2</sup> amine signals are found around 13.5 and 10.0 ppm, respectively. The main difference between the three compounds is the chemical shift of the H-bonded G–H<sup>4</sup> amine proton. Whereas for  $\text{GC}_{\text{H}}$  the G-amine protons are found as a broad coalesced signal at 298 K that splits in two sharp signals at 8.5 (H<sup>4</sup>) and 5.4 (H<sup>5</sup>) ppm below 273 K,<sup>16,18</sup>  $\text{GC}_{\text{Ar}1}$  and  $\text{GC}_{\text{Ar}2}$  showed sharp peaks at room temperature close to 11 ppm. The shape and position of these three H-bonded signals are not sensitive to concentration, temperature, or solvent, indicating strong association in apolar solvents. Additionally, NOESY experiments showed cross-peaks between the H-bonded protons, hence confirming G–C association.

The situation is different in polar solvents such as  $\text{DMSO-D}_6$  or  $\text{DMF-D}_7$  (Figures 2a and S1). The addition of increasing

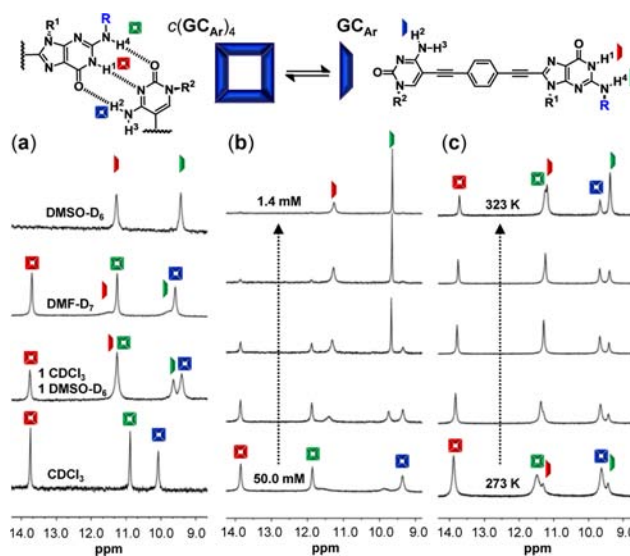


**Figure 2.** Monomer–cyclic tetramer equilibria in polar solvents. Downfield region of the  $^1\text{H}$  NMR spectrum showing the H<sup>1</sup>, H<sup>2</sup> and H<sup>4</sup> signals as a function of (a) solvent nature ( $\text{GC}_{\text{Ar}1}$ ;  $C = \text{ca. } 10^{-2}$  M;  $T = 298$  K), (b) concentration in 1:1  $\text{CDCl}_3/\text{DMSO-D}_6$  ( $\text{GC}_{\text{Ar}2}$ ;  $T = 298$  K), and (c) temperature in 1:1  $\text{CDCl}_3/\text{DMSO-D}_6$  ( $\text{GC}_{\text{Ar}1}$ ;  $C = 10^{-2}$  M).

amounts of  $\text{DMSO}$  to  $\text{CDCl}_3$  solutions of  $\text{GC}_{\text{Ar}1}$  or  $\text{GC}_{\text{Ar}2}$  resulted in the progressive dissociation of the H-bonded species. At the end of these titrations, in 100%  $\text{DMSO-D}_6$ ,  $\text{GC}_{\text{Ar}1}$  or  $\text{GC}_{\text{Ar}2}$  displayed H<sup>1</sup>, H<sup>2</sup>, and H<sup>4</sup> signals at around 11.3, 7.9, and 9.4 ppm, respectively, which are characteristic of monomeric species H-bonded to solvent molecules.

Further experiments were carried out in 100%  $\text{DMF-D}_7$  and a 50%  $\text{CDCl}_3/50\%$   $\text{DMSO-D}_6$  solvent mixture, where we observed a slow equilibrium between two main species: monomer and cyclic tetramer. No other intermediate supramolecular species was detected in these experiments, highlighting the cooperative nature of the cyclic assembly process. Exchange kinetics was studied in more detail by EXSY in  $\text{DMF-D}_7$  (Figure S2), confirming remarkably slow monomer–tetramer exchange processes in all cases. Concentration-dependent experiments within the  $10^{-1}$ – $10^{-3}$  M range afforded the cyclotetramerization constants ( $K_T$ ; Figures 2b and S3), while temperature-dependent experiments in the 323 to 273 K range allowed us to estimate the enthalpic ( $\Delta H$ ) and entropic ( $\Delta S$ ) changes of the assembly process in these polar solvents (Figures 2c and S4). These kinetic and thermodynamic parameters are compared for the 3 compounds in Table 1.

The cyclotetramerization process of  $\text{GC}_{\text{Ar}1}$  and  $\text{GC}_{\text{Ar}2}$  was also studied by absorption, emission, and circular dichroism (CD) spectroscopy in THF as a function of sample concentration and temperature (Figures 3, S5, and S6). As was observed for  $\text{GC}_{\text{H}}$ , when these chiral *N*-arylated monomers associate in macrocycles at high concentrations or low temperatures, a red-shifted absorption shoulder around 395 nm, red-shifted emission maxima, and, significantly, a Cotton CD effect were noticed. The spectroscopic changes monitored in these dilution and cooling experiments were fitted to appropriate models in order to obtain the most relevant thermodynamic parameters in THF ( $K_T$ ,  $\Delta H$ , and  $\Delta S$ ; Figures S5 and S6), which are also listed in Table 1.

The exceptional thermodynamic and kinetic stability of our self-assembled macrocycles, evidenced even in highly polar

**Table 1. Thermodynamic and Kinetic Parameters Calculated for the Cyclotetramerization Process of  $\text{GC}_\text{H}$ ,  $\text{GC}_{\text{Ar}1}$ , and  $\text{GC}_{\text{Ar}2}$  in Different Solvents<sup>10</sup>**

solvent	compd	$K_\text{T}^a/\text{M}^{-3}$	$\Delta H^b/\text{kJ mol}^{-1}$	$\Delta S^b/\text{J mol}^{-1} \text{K}^{-1}$	$\tau^c/\text{s}^{-1}$
1:1 $\text{CDCl}_3/\text{DMSO-D}_6$	$\text{GC}_\text{H}$	$2.9 \times 10^5$	-142	-387	
	$\text{GC}_{\text{Ar}1}$	$7.8 \times 10^5$	-101	-240	
	$\text{GC}_{\text{Ar}2}$	$7.4 \times 10^5$	-93	-224	
DMF- $\text{D}_7$	$\text{GC}_\text{H}$	$2.3 \times 10^5$	-155	-425	3.0
	$\text{GC}_{\text{Ar}1}$	$9.6 \times 10^5$	-86	-190	7.1
	$\text{GC}_{\text{Ar}2}$	$6.4 \times 10^5$	-101	-247	3.8
THF	$\text{GC}_\text{H}$	$1.0 \times 10^{15}$	-225	-465	
	$\text{GC}_{\text{Ar}1}$	$4.6 \times 10^{16}$	-196	-347	
	$\text{GC}_{\text{Ar}2}$	$5.9 \times 10^{16}$	-221	-407	

<sup>a</sup>From dilution experiments (Figures S3 and S5; Table S1). <sup>b</sup>From a van't Hoff analysis of the cooling experiments (Figures S4 and S6; Table S2). <sup>c</sup>From EXSY experiments (Figure S2). A more detailed table including errors and other parameters can be found in the Supporting Information (Table S3).

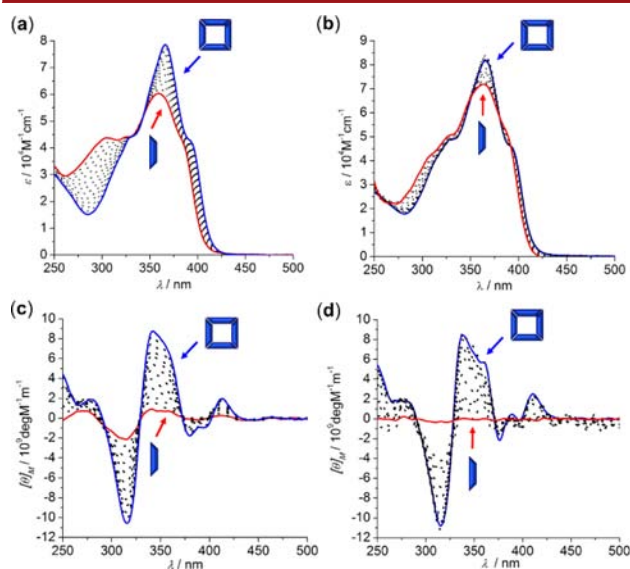


**Figure 3.** Absorption (a,b) and CD (c,d) changes of  $\text{GC}_{\text{Ar}1}$  in THF as a function of temperature ((a,c) from 328 to 273 K;  $C = 1.25 \times 10^{-5}$  M) or the concentration ((b,d) from  $2 \times 10^{-4}$  to  $1 \times 10^{-6}$  M;  $T = 298$  K).

environments, can only be compared with the strongest hydrogen-bonded systems.<sup>19</sup> Monomer–tetramer kinetic exchange is remarkably slow in the NMR time scale and comparable for the three molecules. Such a slow process resembles guanosine exchange in G-quadruplexes, where the nucleobase is also hydrogen-bonded in cyclic complexed systems.<sup>20</sup> Tetramerization constants in DMF or 1:1  $\text{CHCl}_3/\text{DMSO}$  are on the order of  $10^5$ – $10^6$   $\text{M}^{-3}$ , which leads to individual G–C association constants of about 20–30  $\text{M}^{-1}$ . A G–C association constant of 3.7  $\text{M}^{-1}$  was previously determined in polar solvents such as DMSO.<sup>21</sup>

The data presented in Table 1 also reveal that the cyclic tetramers assembled from monomers  $\text{GC}_{\text{Ar}1}$  or  $\text{GC}_{\text{Ar}2}$  are indeed more stable than those of  $\text{GC}_\text{H}$ , affording higher cyclotetramerization constants. In addition, the examination of the NMR and optical spectroscopic trends clearly reveals a higher endurance of  $\text{GC}_{\text{Ar}1}$  or  $\text{GC}_{\text{Ar}2}$  toward dilution or high temperatures.<sup>16</sup> These qualitative observations are translated

into the quantitative  $C_{50}$  and  $T_{50}$  parameters, displayed in Table S3, which stand for the concentration or temperature, respectively, at which half of the molecules are assembled into cyclic tetramers. However, a more careful inspection of the data shown in Table 1 reveals that the origin of such increased stability is not actually coming from a stronger H-bonding of the G unit in the arylated monomers, which would be reflected in a gain in enthalpy upon G–C H-bonding. Instead, such stabilization is mainly caused by the decrease in the absolute value of the entropic term. This effect must be interpreted taking the entire system, including the solvent molecules (DMSO, DMF, THF, and residual  $\text{H}_2\text{O}$ ), as a whole.

Globally, it is clear that tetramerization is driven by an increase in enthalpy due to the formation of 6 G–C H-bonds per monomer in the cyclic assembly.  $\Delta H$  is therefore always negative, and its absolute value increases in less polar solvents (see Table 1). We expected the *N*-arylated products to lead to higher  $\Delta H$  values than  $\text{GC}_\text{H}$ , since the G- $\text{H}^4$  amine proton becomes more acidic and would participate in stronger H-bonds with the C base in the assembly. However, such a G- $\text{H}^4$  proton in the  $\text{GC}_{\text{Ar}1}$  or  $\text{GC}_{\text{Ar}2}$  monomers must also bind strongly to solvent molecules, especially if they are good H-bonding acceptors like DMSO or DMF. This results in the attenuation of this enthalpic effect in these strongly coordinating solvents.

On the other hand, as it is found in most supramolecular systems, the association of 4 molecules leads to the expected negative  $\Delta S$  values. But again we should take into account the solvent molecules, H-bonded to specific sites of the G-unit in reactants and products. Solvation is logically more important in the monomer state, as there is a higher number of available H-bonding donor and acceptor groups, and this introduces some order in the solvation sphere of the monomer. Binding to the C unit upon cyclotetramerization blocks some of these H-bonding groups, and the solvation sphere becomes more disordered in the associated state. This contributes to a milder decrease in entropy upon association, which is again more patent in polar environments, DMSO or DMF, compared to THF. Let us now compare this effect in  $\text{GC}_\text{H}$  and  $\text{GC}_{\text{Ar}1}/\text{GC}_{\text{Ar}2}$ . The presence of the aryl group in  $\text{GC}_{\text{Ar}1}/\text{GC}_{\text{Ar}2}$  leads to different conformations in the monomer state that can be efficiently solvated by the polar molecules. Two of these conformations (A and B) are depicted in Figure 4. Theoretical calculations (DFT; B3LYP/6-31G) select conformation A as being more stable,<sup>16</sup> likely due to steric effects between the amide and aromatic protons in conformation B, the gain in conjugation between pyrimidine and phenyl rings, and the formation of an intramolecular H-bond between the *ortho*-aryl proton and the G- $\text{N}^3$  lone pair. Now, when  $\text{GC}_{\text{Ar}1}/\text{GC}_{\text{Ar}2}$  associate, H-bonding to C necessarily fixes conformation A and this produces a sterically crowded region around the Watson–Crick pair that heavily hampers solvation. Hence, we think that the solvation sphere around the  $\text{GC}_{\text{Ar}1}/\text{GC}_{\text{Ar}2}$  tetramers suffers a higher alteration than that of  $\text{GC}_\text{H}$  upon cycle formation, resulting in smaller  $\Delta S$  values in polar solvents.

In short, although the differences are not very large, the presence of the electron-poor aryl substituents at the G- $\text{N}^2$  amino group increases the stability of the tetrameric macrocycles, which arise as the main supramolecular product even in polar environments or low concentrations where H-bonding self-assembly is considerably weakened. From the thermodynamic parameters extracted from NMR and optical spectroscopy experiments in solvents of different polarity, we noted a

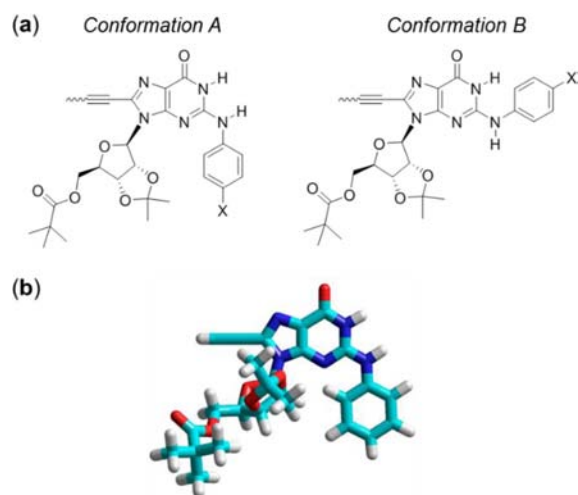


**Figure 4.** (a) Structure of two possible conformations (A and B) for the aryl group in  $GC_{Ar1}/GC_{Ar2}$ . (b) Energy minimized structure (DFT; B3LYP/6-31G) obtained for an arylated G model.

subtle interplay between enthalpic and entropic effects that involve not only the  $GC_H$  or  $GC_{Ar1}/GC_{Ar2}$  supramolecular systems but also their solvent coordination sphere.<sup>22</sup>

## ■ ASSOCIATED CONTENT

### Supporting Information

Experimental procedures and characterization data,  $^1H$  and  $^{13}C$  NMR spectra, and HRMS for novel compounds. NMR, spectroscopic UV-vis, and CD data as a function of temperature and concentration along with the methods employed to analyze the monomer-cyclic tetramer equilibrium (thermodynamic and kinetic parameters). The Supporting Information is available free of charge on the ACS Publications website at DOI: 10.1021/acs.orglett.5b01042.

## ■ AUTHOR INFORMATION

### Corresponding Author

\*E-mail: david.gonzalez.rodriguez@uam.es.

### Notes

The authors declare no competing financial interest.

## ■ ACKNOWLEDGMENTS

Funding from the European Research Council (ERC-StG 279548) and MINECO (CTQ2011-23659) is gratefully acknowledged.

## ■ REFERENCES

- (1) (a) *Macrocyclic Chemistry. Current Trends and Future Perspectives*; Gloe, K., Ed.; Springer: Dordrecht, 2005. (b) *Modern Supramolecular Chemistry. Strategies for Macrocyclic Synthesis*; Diederich, F., Stang, P. J., Tykwinski, R. R., Eds.; Wiley-VCH: Weinheim, 2008.
- (2) Kudernac, T.; Lei, S.; Elemans, J. A. A. W.; De Feyter, S. *Chem. Soc. Rev.* **2009**, *38*, 402.
- (3) (a) Gong, B.; Shao, Z. *Acc. Chem. Res.* **2013**, *46*, 2856. (b) Shimizu, L. S.; Salpage, S. R.; Korous, A. A. *Acc. Chem. Res.* **2014**, *47*, 2116.
- (4) Iyoda, M.; Yamakawa, J.; Rahman, M. J. *Angew. Chem., Int. Ed.* **2011**, *50*, 10522.
- (5) Dong, Z.; Luo, Q.; Liu, J. *Chem. Soc. Rev.* **2012**, *41*, 7890.
- (6) Gokel, G. W.; Negin, S. *Acc. Chem. Res.* **2013**, *46*, 2824.
- (7) Höger, S. *Angew. Chem., Int. Ed.* **2005**, *44*, 3806.

(8) Ballester, P.; de Mendoza, J. In *Modern Supramolecular Chemistry. Strategies for Macrocyclic Synthesis*; Diederich, F., Stang, P. J., Tykwinski, R. R., Eds.; Wiley-VCH: Weinheim, 2008; p 69.

(9) (a) Hunter, C. A.; Anderson, H. L. *Angew. Chem., Int. Ed.* **2009**, *48*, 7488. (b) Ercolani, G.; Schiaffino, L. *Angew. Chem., Int. Ed.* **2011**, *50*, 1762.

(10) Montoro-García, C.; Camacho-García, J.; López-Pérez, A. M.; Bilbao, N.; Romero-Pérez, S.; Mayoral, M. J.; González-Rodríguez, D. *Angew. Chem., Int. Ed.* **2015**, DOI: 10.1002/anie.201501321.

(11) For metallosupramolecular cyclic tetramer assemblies, see: (a) Würthner, F.; You, C.-C.; Saha-Möller, C. R. *Chem. Soc. Rev.* **2004**, *33*, 133. (b) Hwang, I.-W.; Kamada, T.; Ahn, T. K.; Ko, D. M.; Nakamura, T.; Tsuda, A.; Osuka, A.; Kim, D. *J. Am. Chem. Soc.* **2004**, *126*, 16187.

(12) For other H-bonded cyclic tetramer assemblies in solution, see: (a) Nuckolls, C.; Hof, F.; Martín, T.; Rebek, J., Jr. *J. Am. Chem. Soc.* **1999**, *121*, 10281. (b) Ohkawa, H.; Takayama, A.; Nakajima, S.; Nishide, H. *Org. Lett.* **2006**, *8*, 2225. (c) Orentas, E.; Wallentin, C.-J.; Bergquist, K.-E.; Lund, M.; Butkus, E.; Wärnmark, K. *Angew. Chem., Int. Ed.* **2011**, *50*, 2071. (d) Yang, Y.; Xue, M.; Marshall, L. J.; de Mendoza, J. *Org. Lett.* **2011**, *12*, 3186.

(13) For the use of nucleobases in supramolecular chemistry, see: (a) Sivakova, S.; Rowan, S. J. *Chem. Soc. Rev.* **2005**, *34*, 9. (b) Sessler, J. L.; Lawrence, C. M.; Jayawickramarajah, J. *Chem. Soc. Rev.* **2007**, *36*, 314.

(14) Camacho-García, J.; Montoro-García, C.; López-Pérez, A. M.; Bilbao, N.; Romero-Pérez, S.; González-Rodríguez, D. *Org. Biomol. Chem.* **2015**, *13*, 4506.

(15) (a) Hartwig, J. F. *Acc. Chem. Res.* **1998**, *31*, 852. (b) Yang, B. H.; Buchwald, S. L. *J. Organomet. Chem.* **1999**, *576*, 125.

(16) See the Supporting Information for further details.

(17) Protection of the G-carbonyl group was found to be essential to perform palladium catalyzed couplings on bromoguanosines efficiently. See ref 11 and: (a) Western, E. C.; Shaughnessy, K. H. *J. Org. Chem.* **2005**, *70*, 6378. (b) Zerdan, R. B.; Cohn, P.; Puodziukynaite, E.; Baker, M. B.; Voisin, M.; Sarun, C.; Castellano, R. K. *J. Org. Chem.* **2015**, *80*, 1828.

(18) (a) González-Rodríguez, D.; van Dongen, J. L. J.; Lutz, M.; Spek, A. L.; Schenning, A. P. H. J.; Meijer, E. W. *Nat. Chem.* **2009**, *1*, 151. (b) González-Rodríguez, D.; Janssen, P. G. A.; Martín-Rapún, R.; De Cat, I.; De Feyter, S.; Schenning, A. P. H. J.; Meijer, E. W. *J. Am. Chem. Soc.* **2010**, *132*, 4710.

(19) Blight, B. A.; Hunter, C. A.; Leigh, D. A.; McNab, H.; Thomson, P. I. T. *Nat. Chem.* **2011**, *3*, 244.

(20) Davis, J. T.; Kaucher, M. S.; Kotch, F. W.; Iezzi, M. A.; Clover, B. C.; Mullaugh, K. M. *Org. Lett.* **2004**, *6*, 4265.

(21) Newmark, R. A.; Cantor, C. R. *J. Am. Chem. Soc.* **1968**, *90*, 5010.

(22) Amenta, V.; Cook, J. L.; Hunter, C. A.; Low, C. M. R.; Sun, H.; Vinter, J. G. *J. Am. Chem. Soc.* **2013**, *135*, 12091.